

15TH ANNUAL SUMMER PROGRAM
SYMPOSIUM ON
QUANTITATIVE METHODOLOGY IN LIPID RESEARCH.
PART III.

conducted by The American Oil Chemists' Society
at Pennsylvania State University, University Park, August 3-7, 1964

Under the sponsorship of the Education Committee, N. H. KUHRT, Chairman,
and GEORGE ROUSER, Program Chairman

Study of Biological Structure at the Molecular Level with
Stereomodel Projections. II. The Structure of Myelin in
Relation to Other Membrane Systems

F. A. VANDENHEUVEL, Animal Research Institute, Research Branch, Canada Department of Agriculture,
Ottawa, Ontario

BIOLICAL STRUCTURES, such as membranes, result from the cooperative association of molecules united by forces of cohesion. In spite of a considerable variety of participant molecular species, such structures display a stability which cannot be explained unless it is assumed that the constituent molecules adopt configurations that allow for close approach and alignment favoring cohesion. This assumption, which suggests the existence of precise configurational relationships is supported by a rapidly growing sum of evidence. Structural investigations at the molecular level could not be conclusive, therefore, without the study of accurately built models from which satisfactory estimations of cohesive forces can be made. In this work, accuracy is invaluable in permitting one to detect unerringly, and to reject unreservedly, situations which might otherwise have appeared possible.

The physical state of molecules in membranes is clearly a matter of importance in relation to their probable configurations. Here one is tempted to draw conclusions from apparent analogies with simple models studied by physicists. The unique properties of membrane systems should caution, however, against indiscriminate extrapolations of the related data. X-ray diffraction and electron microscopic observations,

optical properties such as birefringence, the specificity of functions and of the related enzymic and immunochemical reactions, all clearly indicate a molecular order in membranes which is foreign to the bulk liquid state. Association to a relatively high mol wt structural protein should even deny the lipids a degree of freedom comparable to that found in smectic liquid-crystals or in monolayers. In fact, the multiplicity of constituent molecular species in membranes would seem to constitute the main difference with a truly crystalline organization which membranes mimic in many other ways. For lack of a more specific term, the situation may be called "para-crystalline."

Undoubtedly, the very existence and the stability of biological structures depend on the development of high intermolecular cohesive forces. Thus the most probable configurations of individual components should correspond to the most favorable overall force situation. A study of models generally reveals that this situation is best achieved when molecules adopt relaxed, uncomplicated configurations corresponding to a low energy level. As any biological structure, a membrane may be considered as a molecular ecology deriving both structural and functional specificity from the properties and arrangement of constituent

INDEX

- | | | | |
|---------|---|---------|---|
| 481-492 | STUDY OF BIOLOGICAL STRUCTURE OF THE MOLECULAR LEVEL WITH STEREOMODEL PROJECTIONS. II. The Structure of Myelin in Relation to Other Membrane Systems, by F. A. Vandenheuvel | 504-511 | ARACHIDONIC, 5, 11, 14, 17-EICOSATETRAENOIC AND RELATED ACIDS IN PLANTS—IDENTIFICATION OF UNSATURATED FATTY ACIDS, by Hermann Schlenk and Joanne L. Gellerman |
| 492-500 | LIPID CLASS AND FATTY ACID COMPOSITION OF INTACT PERIPHERAL NERVE AND DURING WALLERIAN DEGENERATION, by J. F. Berry, W. F. Cevallos and R. R. Wade, Jr. | 511-516 | POSITIONAL ISOMERISM OF UNSATURATED FATTY ACIDS IN THE RAT QUANTIFICATION OF ISOMERIC MIXTURES, by D. Sand, N. Sen and H. Schlenk |
| 500-504 | HUMAN PLATELET LIPIDS AND THEIR RELATIONSHIP TO BLOOD COAGULATION, by Aaron J. Marcus and Dorothea Zucker-Franklin | 516-528 | DIETARY FAT AND THE FATTY ACID COMPOSITION OF TISSUE LIPIDS, by K. K. Carroll |

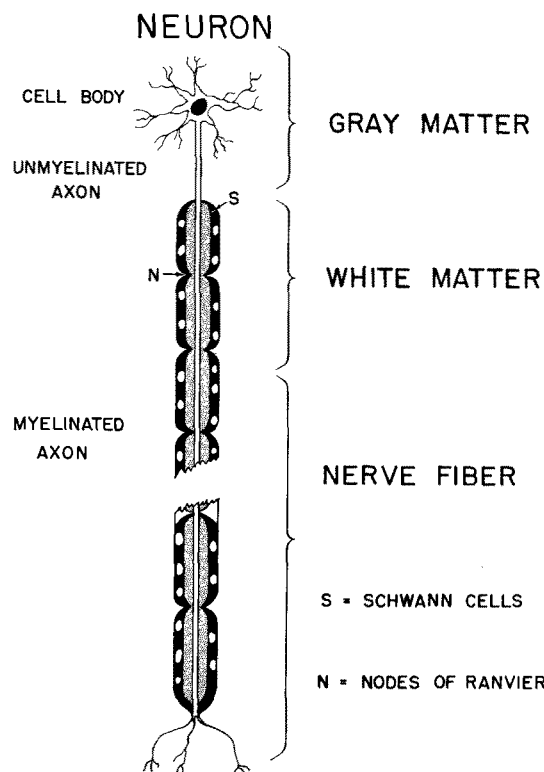


FIG. 1. Diagram of peripheral neuron. Myelin is layer adjacent to central tubular axon. Actual nerve is cable-like formation comprising many parallel fibers in single envelope.

molecules. The common and complementary structural features which constitute the "raison d'être" of a stable ecology must provide a key to its elucidation. Their discovery could lead, therefore, to representative models to which multiple correlations with existing data should confer a high degree of probability.

Data used in guiding this type of investigation vary considerably in significance. The material of choice includes the chemical constitution of constituents, when it comprises the stereoconfigurations; X-ray data, when obtained with fresh, unfixed tissues; unbiased analytical data; optical properties such as birefringence, when it clearly indicates on orientation of molecules; chemical and physical properties of components, particularly when observed under comparable conditions. Electron microscopic observations are only of value when structural alterations due to fixation and embedding have been studied and their extent estimated, by X-ray diffraction, for instance. Only in such case do they provide meaningful correlations.

In previous communications (1,2), the author has outlined methods for handling stereomodels, for the calculation of forces, and for the production and uses of truly representative diagrams. It must be emphasized that one can only hope to represent the most probable arrangement of molecules in equilibrium situations, since biological structures are continuously disturbed to some extent by forces of thermal and ionic origin. In the present communication a summary of previous work on myelin (1,3) will be used as a background to discuss aspects of the problem which are of interest to other membrane systems.

Myelin

From the nerve cell, or neuron, extends a long tubular process, called axon (Figure 1). This is covered over most of its length by the myelin sheath.

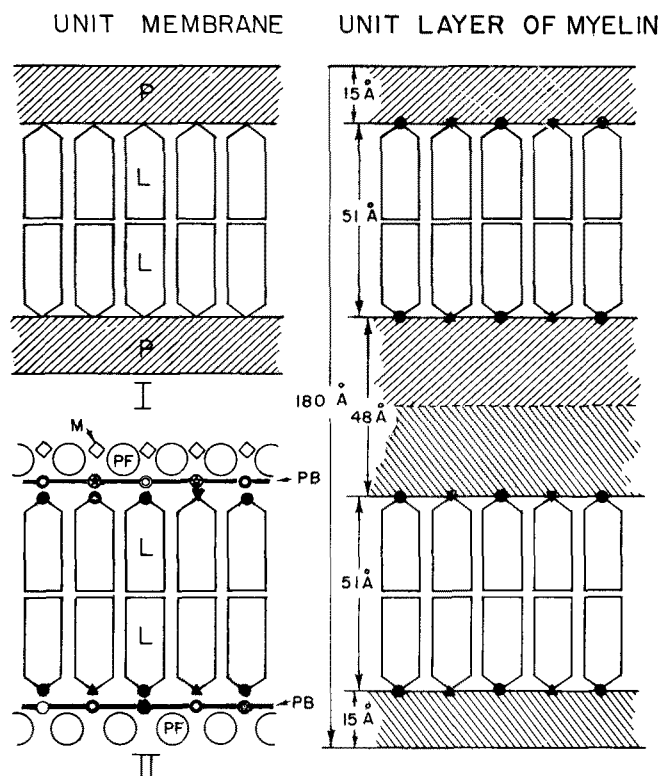
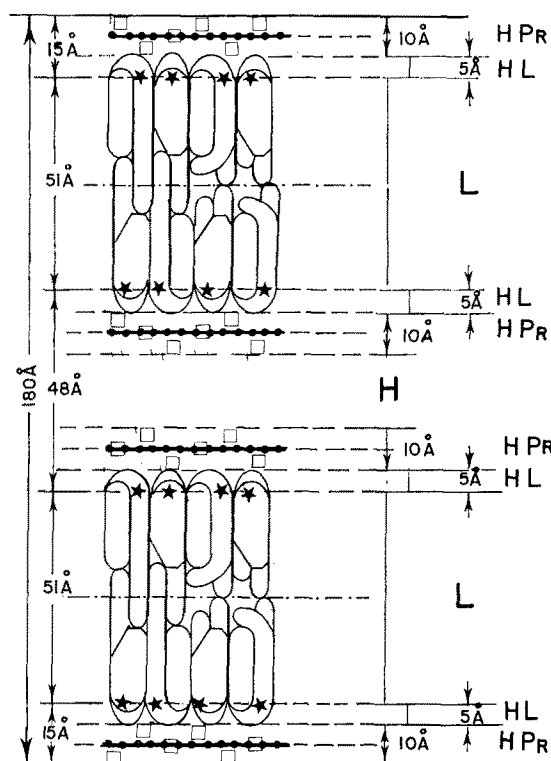


FIG. 2. Membrane systems. Stars, triangles, circles, etc., symbolize diversity of functional groups on protein and lipids. I. The Danielli concept of membrane structure: P, hydrated protein; L, lipid in bimolecular leaflet. II. Simplified diagram of a complete membrane: PB, structural protein, L,L, lipids in the "lipoprotein barrier" unit; PF, functional protein (enzymes and other proteins of the superstructure); M,M, mucopolysaccharides and other non protein components. III. The unit layer of myelin in rat sciatic nerve, from the data obtained by Finean (9).

The latter is generated by satellite cells, the Schwann cells S in peripheral nerve, located at regular interval along the myelinated nerve. As the electron microscopic view of a section shows in Figure 12, ref. 1, the myelin sheath is a multilayered structure. It is important to remember that each of the layers is made from two satellite cell membranes. This is explained by Figure 11, ref. 1, showing the progress of myelination first demonstrated by Geren (4) and later by Robertson (5). The axon is first invaginated in the satellite cell and wrapping of the cell membrane occurs jelly-roll fashion. It can be seen that two layers of the cell membrane, united by their outer surfaces, form the unit layer of myelin. At the right of Figure 2, a diagram of the unit layer shows a wider central portion corresponding to this junction separating two identical membrane components.

About 40% of the white matter of brain is myelin (8) which has been recently isolated in a pure, structurally intact form by several independent workers (6-8). We are indebted to Finean (9) for accurate low-angle X-ray diffraction measurements of the distance separating the structural elements of the unit layer. The density curves shown in Figure 13, ref. 1, display maxima interpreted as the positions of electron-dense phosphorus atoms in the phospholipids arranged tail to tail. In all cases the phosphorus to phosphorus distance was about 50 Å, a fact confirmed by a recent, more refined analysis, (10). Analytical data on pure myelin (8), reveal little else than lipid, protein, water and ions. Finean's results thus clearly indicate that a hydrated protein must lie on both sides of a bimolecular lipid leaflet,



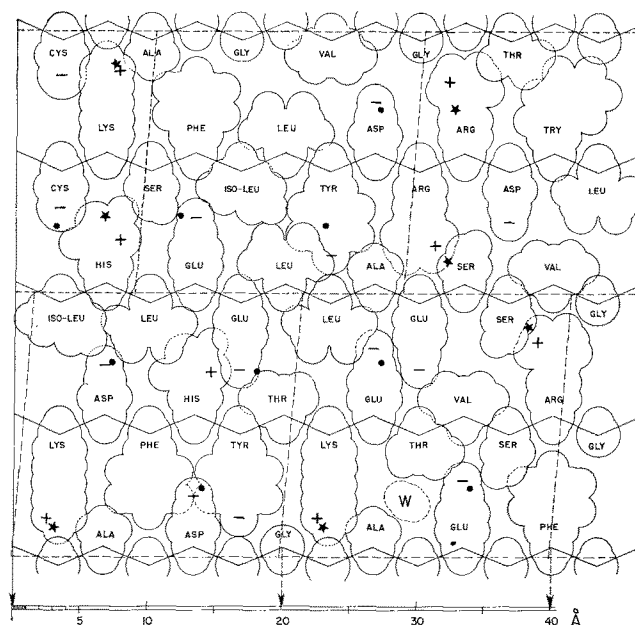
★ P, IN PHOSPHOL. → AMIDE GROUPS. □ AMINO AC. RES.

FIG. 3. Radial section through unit layer of myelin of rat sciatic nerve (cf. Fig. 2, III) showing arrangement of cholesterol-lipid complexes L, hydrated protein layer HPr, and hydrated, polar layer of the lipids, HL. Intraperiod region H is occupied by water molecules.

thus confirming the early hypothesis of Danielli (11) (Figure 2, I). This is entirely consistent with the radial orientation of lipids demonstrated by birefringence (12,13) and with hydrophilic properties of the polar lipids demonstrated by countless independent observations. The problem in the case of myelin consisted of finding a tail to tail arrangement accounting for the 50 Å phosphorus to phosphorus distance, yet permitting the fitting of hydrocarbon tails varying in length from 17 to 37 Å and containing from 0 to 3 double bonds. It also included the arrangement of the observed proportion (8) of protein within a 10 Å-wide layer.

The Lipids of Myelin

Myelin lipids other than cholesterol can adopt one of two very similar configurations suggested by Figure 15, ref. 1. One is characteristic of phosphoglycerides, the other of sphingolipids. Both are obtained when hydrocarbon chains, those of the fatty acids in phosphoglycerides and those of the fatty acid and sphingosine in sphingolipids, adopt what may be called a zig-zag, strainless configuration (1). The chains can then be brought in close contact up to the ninth carbon atom from the carboxyl group in all cases. When the common characteristic sequence of the polar chain, indicated in heavy line, also adopts this type of configuration, that of the whole molecule is entirely determined. In this configuration the molecule can associate with a molecule of cholesterol. Figure 16, ref. 1, describes a cholesterol-lecitin complex typical of phosphoglycerides. The fit of the cholesterol molecule is excellent regardless of the polar group carried by the polar chain, and regardless of chain length and extent of unsaturation. The stability of the resulting complex is predicted by



PROTEIN LAYER

★, P, IN $\rightarrow PO^-$; •, N IN $-NH^+$ AND $-N(CH_3)^+$ OF UNDERLYING PHOSPHATIDES

FIG. 4. Diagram obtained by superimposing on parallelograms in Fig. 22, ref. 1 (dashed lines) peptide chains in the β keratin, parallel configuration (cf. Fig. 24 in ref. 1). Amino acid composition of protein is approximately that found in myelin (Table I). The sequences are arbitrary.

London-van der Waals force calculation (1) and its cross-sectional area corresponds to complexes obtained in mixed monolayer studies (14,15). These conclusions also apply to sphingolipid complexes such as the cholesterol-sphingomyelin complex (Figure 17, ref. 1). As Figure 22, ref. 1 shows, there are dissimilarities in end view contours and in polar group coordinates between the P complex of phosphoglycerides and the S complex of sphingolipids. However, the perfect alignment of groups in complexes arranged in the manner described, clearly demonstrates that the two types have important common elements of symmetry. Phosphoglyceride complexes each contain at least one palmitic or oleic acid chain (1). Counting from the phosphorus atoms, both chains have the same effective length, 25.5 Å. Thus the simple tail to tail abutment of such units always produces the correct phosphorus to phosphorus distance. With sphingolipid complexes, interlocked units (Figure 18, ref. 1) are formed by tail interdigitation characterized by strong London-van der Waals interaction. Such units are the most abundant, and should constitute key structural elements of normal myelin (1). Both arrangements are illustrated in Figure 19 and 20, ref. 1. In Figure 19, ref. 1, complexes of all types are described by simplified models which are nevertheless exactly to scale as regards critical dimensions. Figure 20, ref. 1, shows the models assembled to give the correct phosphorus to phosphorus distance in the radial, rod-like arrangement predicted by birefringence.

The Protein of Myelin

Results on the amino acid composition of pure myelin protein published by Huleher (6) were converted to per cent amino acid residue composition (Table I). The average residue mol wt was then combined to accurate protein to lipid class ratios obtained by Norton and associates (8), yielding a lipid area per amino acid of 32.5 Å² (3).

In pure myelin, 77.7% lipid and 22% protein

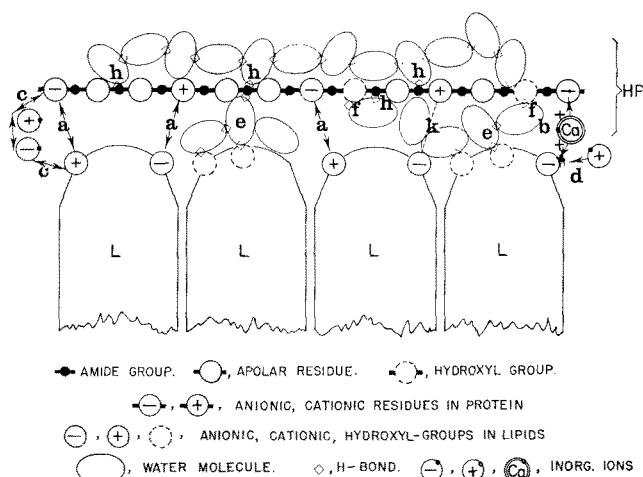


FIG. 5. Schematic description of forces in lipoprotein layer (radial section). Cf. text.

account for 99.7% of the dry matter. Only protein could play the organizing role, extending its stabilizing influence over relatively large areas much in the manner of the warp in cloth. Thus an arrangement of protein chains was sought whereby the whole surface of the lipids could be covered. Only the chain arrangement found in the parallel β keratin model (16) in the plane perpendicular to the pleated sheet (Figure 24, ref. 1) was found to fulfill the requirements. In this configuration, each amino acid occupies 32.5 \AA^2 (9.8×3.32) area and the thickness of a single layer is close to 10 \AA (3) exactly as required.

The Structure of Myelin

Figure 4 shows a diagram representing the unit layer in rat sciatic myelin (9). It includes a 10 \AA layer of hydrated protein HPr on both sides of bimolecular lipid leaflets L. The outside protein layers of the unit are in van der Waals contact with the lipids and with protein layers of adjacent unit layers. In intraperiod region H, protein layers are separated by about 6 molecules of water. X-ray dimensions on the left side are seen to correspond to the proposed model. Myelin water content, calculated from the latter, corresponds to the data obtained by Finean (17). Species differences in unit layer repeat (9) can be ascribed to specific amounts of water in the intraperiod region H (3). The absence of water in this region corresponds in this model to a 160 \AA unit. This dimension is obtained at the critical stage of dehydration revealed by Finean's extensive study (18). The present model thus explains irreversible changes caused by dehydration beyond the critical stage since the protein layers would then become entangled under pressure. These, and other correlations with experimental data have been fully described (3).

Cohesional Forces in Membranes

The cohesional forces at play could now be examined with more confidence. The diagram shown in Figure 22, ref. 1, reveals a characteristic pattern where each parallelogram contains four cholesterol-lipid complexes. The diagram in Figure 4 was obtained by superimposing on the lipid diagram indicated in dashed lines, that of protein chains in the proposed configuration and bearing amino acid residues in proportion to the composition found by Hulcher (6) as described in Table I. Each of the

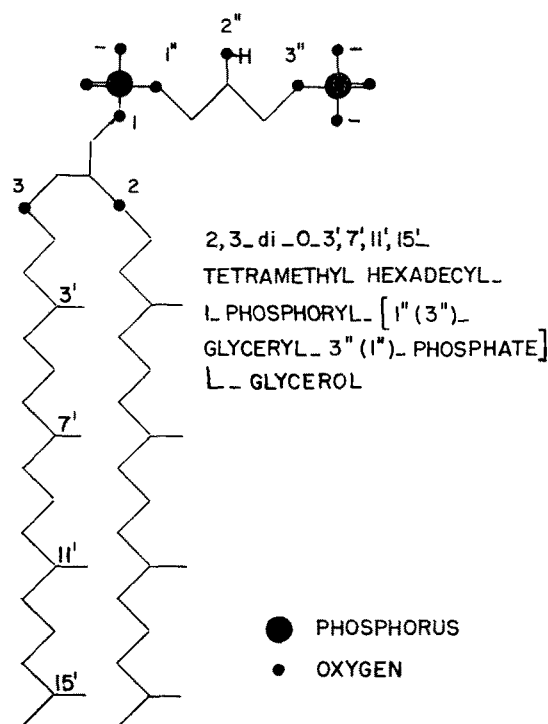


FIG. 6. The major lipid in *Halobacterium cutirubrum* (19).

parallelograms in the lipid pattern exactly corresponds to 12 amino acid residues.

London-van der Waals interactions must obviously contribute to the cohesion of this relatively crowded protein system. What is more evident however, is the constellation of charges both on lipids and protein. Long range coulombic attractions not necessarily leading to salt formation must therefore be expected. However, as the steromodel shows, some of these interactions can easily take place between amino acid chains in adjacent chains, thus undoubtedly competing with the lipid-protein ionic binding suggested by the coincidence of + and - signs in amino acids with the stars and dots in underlying lipids. What the diagram does not show are numerous water molecules providing their own contribution to the stability of the system through hydrogen bonding.

This is schematically represented in Figure 5 showing a vertical section through the lipids L, and the hydrated protein HP where water molecules are approximated by ellipses. The system of forces binding lipids and proteins comprises important London-van der Waals interactions between lipids. Lipid-protein binding involves coulombic attraction between opposite charges, exemplified in a, and ionic binding of negative charges by Ca ions, exemplified in b. Competition by small ions is illustrated in c and d, while the screening effect of highly dielectric water molecules is exemplified in k. Completing the picture are many water molecule bridges between all groups susceptible of hydrogen binding.

From preliminary estimations it is clear that the available cohesional energy is sufficient to account for the stability of the system. Much more difficult to establish are the relative contributions of component forces in this highly competitive system, without precise information about the structure of the water network. It is clear that one should expect to find membrane systems more specifically oriented toward one of the binding modes just described. Consider, for example, the situation in the membrane of the strange bacteria, *Halobacterium cutirubrum*

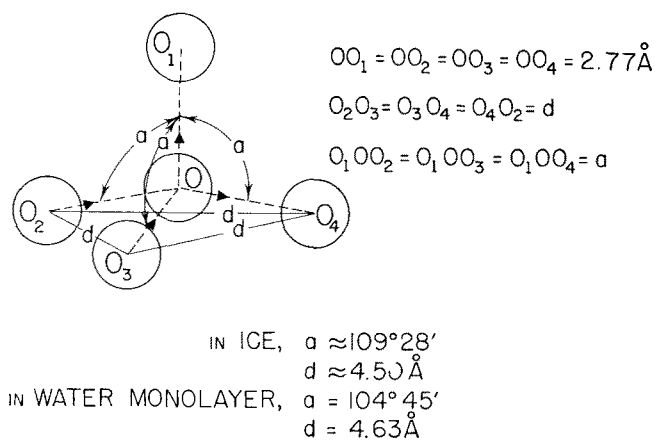


Fig. 7. Water lattice parameters in ice and in water monolayer.

which thrives in 4 M NaCl media. About 90% of the lipids are accounted for by the phosphatide described in Figure 6. This constitution, recently established by Kates (19) indicates negative charges only. The protein, recently analyzed by Kushner (20) shows a very large excess of negative charges. The bacterium survives presumably because most of the negative charges are neutralized by cations. However, the free lipid does not appreciably bind cations when placed in water or even in 4 M NaCl solutions. Some structural device in the membrane must permit cation binding by negative charges, thus preventing the membrane dissociation which actually occurs when the medium is diluted below 2 M (20). One must also explain why the membrane mainly uses potassium for this purpose in a culture medium heavily loaded with sodium ions. These and many questions of general interest to membrane research appear to be answered by the following considerations of the properties of water.

Water in Membranes

Water Monolayer

Water, or its constituent atoms, are key reactants in many metabolic pathways. This is why, throughout the course of a long evolution, living organisms have maintained a close association with the medium in which all originated. Hence, in the selection of viable biological architectures, the properties of water have had a relentless and decisive influence, and water molecules became inescapable components of biological structures. Very little is known about the multiple roles of structural water. "Biology," wrote Szent-Györgyi, "may have been unsuccessful in understanding the most basic functions because it focussed its attention only on the particulate matter, separating it from its two matrices, water and the electromagnetic field" (21).

A few years ago, following an article by the same author (22), several scientists began to wonder how enzymatically produced energy could be transported. In the case of membranes, the question was pertinent since, aside from the mitochondrial membrane studied by Green and Fleischer (23), and Fernandez-Moran (24), there exist countless others which are not richly endowed in recognizable electron transfer systems yet utilize energy supplied by a few ATPase molecules to drive mechanisms spread over their entire surfaces. The long distance tangential energy transfer this situation suggests could hardly use bulky ions as energy carriers. Protons or electrons moving along suitable conductive paths would be much more efficient.

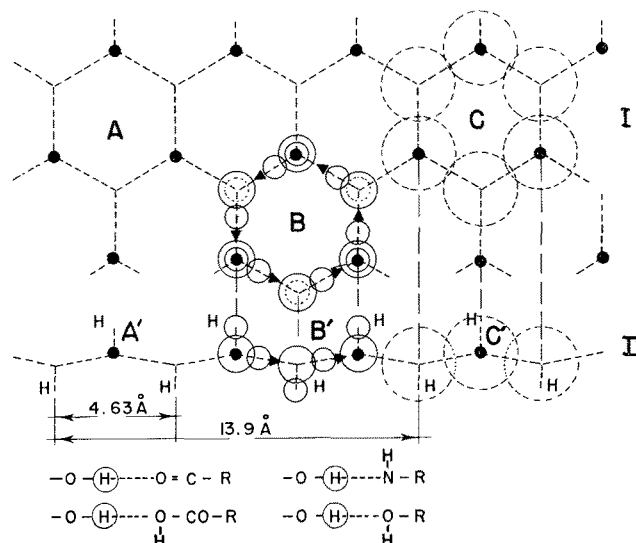


Fig. 8. Plan (I), and elevation (II) of water monolayer. Centers of water molecules (oxygens) which have hydrogen atom pointing above the median plane of the monolayer are indicated by small solid circles. The distance between amino acid side chains in β keratin antiparallel configuration is about 3.5 Å; hence $4 \times 3.5 \text{ \AA} = \text{approx. } 3 \times 4.63 \text{ \AA} = \text{EF} = 13.9 \text{ \AA}$.

Work on the conductivity of proteins has shown (25-29) that these membrane constituents, lacking a continuous conjugated system of double bonds, are poor conductors in the dry state. Some, among which is keratin (26), will become appreciably more conductive when a sufficiently extended water film is adsorbed at their surfaces. The number of water molecules thus involved (25), represents from two to three times the number of polar groups. This suggests the formation of a monolayer consisting of water molecules adsorbed on the polar groups and of interconnecting water molecules. The observed conductance then could be that of water, the role of the protein being that of a structural support. Proton transfer through the mechanism described by Eigen (30) would appear the more probable process (25). An amplification of this theory by Klotz (31) describes an ice-like water network transporting protons or electrons bucket-brigade fashion over relatively long distances. The fit of water molecules in the ice lattice explains how proton transfer could be faster than in liquid water, being in fact, only from two to three orders of magnitude slower than the flow of electrons in metals (30). The characteristic ice lattice parameters could not however, exist in a monolayer since the modification of the $104^\circ 45'$ H-O-H angle found in water (32-34) to the tetrahedral $109^\circ 28'$ found in ice (35) is only justified by the large increase in cohesion arising from the three-dimensional ice lattice symmetry.

The proposed arrangement for the water monolayer is best understood by first considering that in ice (Figure 7), each oxygen atom is equidistant from four neighbors, and all angles a are about equal to the tetrahedral dimension. The hydrogen atoms of the central water molecule are located along OO_1 and OO_4 and each of its two lone electron pairs is directed towards one of the two neighboring oxygen atoms, O_2 and O_3 . The latter in turn direct one of their two hydrogen atoms towards the central oxygen atom. Hence a balanced system of hydrogen bonds is established, the hydrogen bond distance being 2.77 Å (36). In the proposed monolayer arrangement, the H-O-H angle in liquid water, $104^\circ 45'$, is maintained and any water molecule is symmetrically connected by 2.77 Å

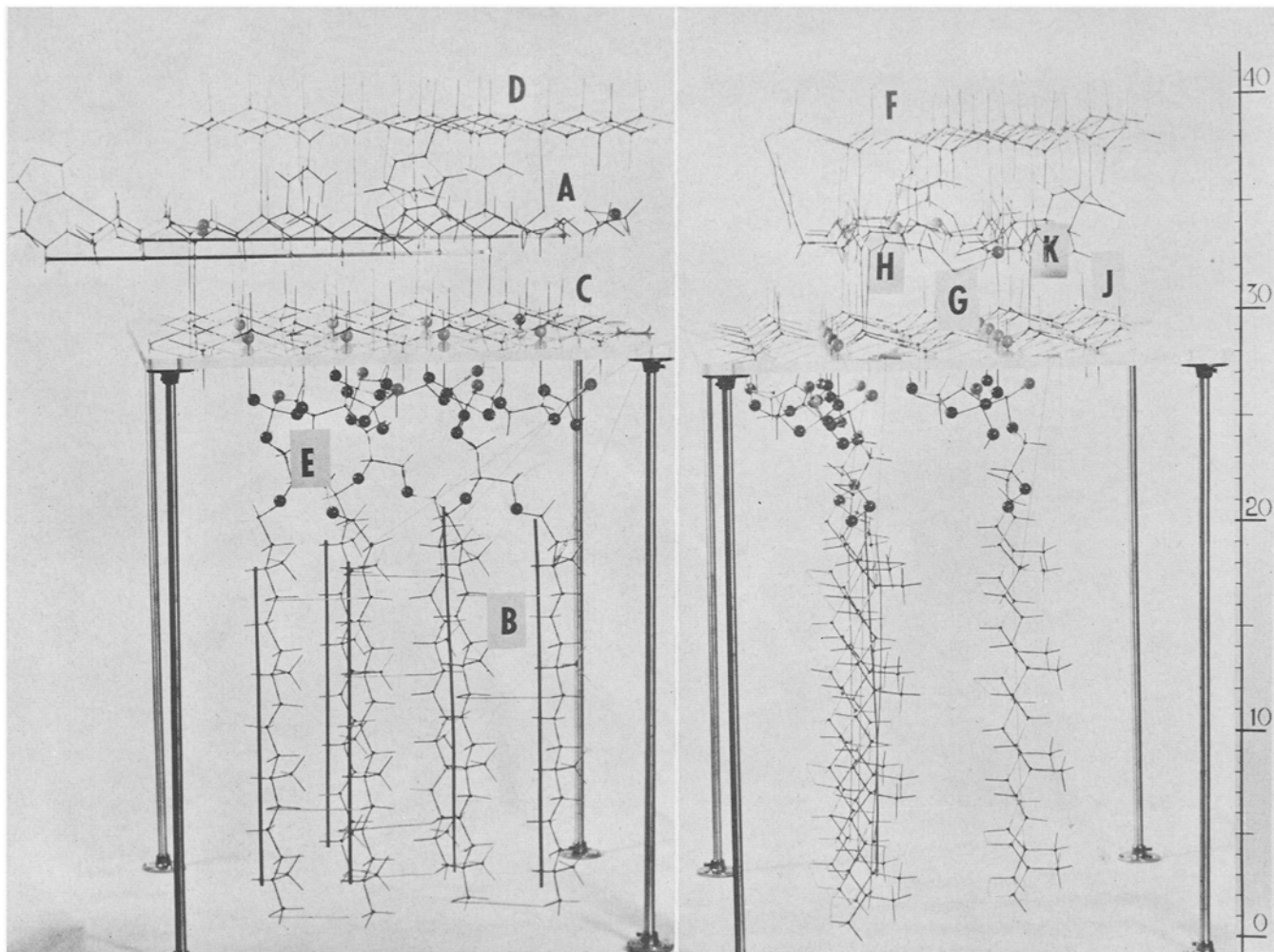


FIG. 9 (left) and FIG. 10 (right). Two views of Dreiding model of part of *Halobacterium cutirubrum* membrane. The protein layer (A in Fig. 9, HKJ in Fig. 10) is in the β keratin antiparallel configuration. The amino acids are connected by H bonds to top water monolayer (D in Fig. 9, F in Fig. 10) and also to cation-water monolayer (C in Fig. 9, G in Fig. 10). In the latter, cations are represented by rows of light gray spheres of arbitrary diameter resting on Plexiglass support. This layer is ionically linked through the cations to lipids B (cf. Fig. 11). Dark spheres of arbitrary diameter in polar region E (Fig. 9) represent an extensive system of oxygen atoms (cf. Fig. 6). Most of the latter actually are tangent to their nearest oxygen neighbors (van del Waals boundaries).

hydrogen bonds to three neighbors only. This leaves one hydrogen atom per molecule not engaged in hydrogen bonding. Figure 8 shows, both in plane I and elevation II, in A and A', the simple hexagonal lattice, in B and B', the atoms with their covalent radii, and in C and C', the van der Waals radii of oxygen atoms. Elevation II shows the free hydrogen atoms projecting vertically and alternately above and below the medium plane of a monolayer about 2.5 Å-thick. This arrangement, one among others, is particularly interesting in that the distance d between "free" hydrogen atoms, 4.63 Å, exactly corresponds to parameters of proteins, the β keratin chain in antiparallel configuration, for example. Furthermore, it is the broadest cross-sectional dimension of a fatty acid chain (21). Thus either proteins or lipids could be involved with the "free" hydrogen atoms of the water monolayer through several forms of hydrogen bonding exemplified at the bottom of Figure 8. Furthermore, the monolayer could readily serve as a common ground for the adsorption of both compounds.

Figure 9 represents the model of a portion of the membrane in *Halobacterium cutirubrum*. In this model the protein chains, A, were given the β keratin, antiparallel mode configuration, and the top water layer, D, was given the monolayer configuration just described. It will be shown in more detail in a forth-

coming publication, that all polar chains of the protein can be connected through hydrogen bonds to water molecules of the monolayer. They can do this, some of them in several ways, without strain, distortion or steric hindrance. Furthermore, the carboxyl moiety in amide groups can do this also. Thus the possibility exists for such protein to coordinate a water monolayer of the type suggested by the studies on water adsorption and protein conductivity discussed above. The protein is also shown adsorbed to monolayer C (see also G in Figure 10). This is the conductive, K-selective water-cation monolayer which will now be described.

Conductive, K-Selective Water-Cation Monolayer

The disoriented pattern of dipoles indicated by the stereomodel of water monolayer D, Figure 9, would lead to appreciable charge dispersion. It is not surprising therefore that the observed increase in "protein" conductivity is a relatively modest one. However, as Figure 11 demonstrates, a highly directional arrangement is obtained when some of the water molecules are replaced by positively charged particles such as in rows A and B. Thus along horizontal row C, all positive flows, indicated by arrows, point in the same direction, and the system should be highly conductive. Of course, the positive particles could be

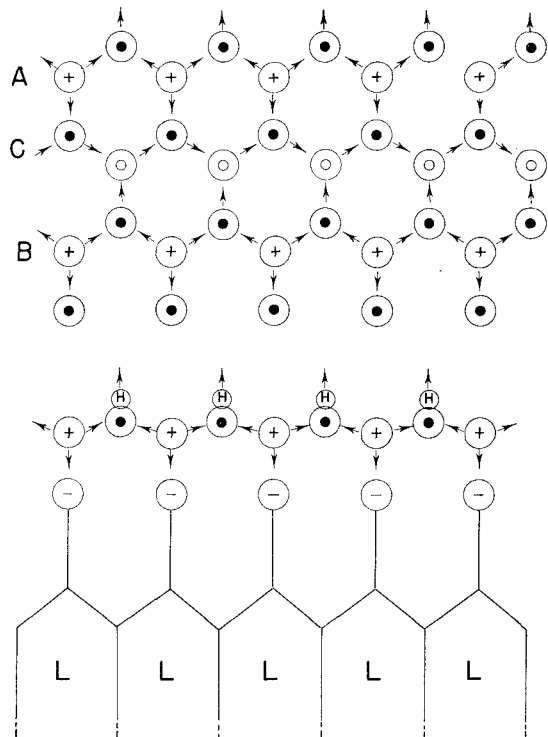


FIG. 11. Plan (top) and elevation (bottom) of conductive cation-water monolayer. Elevation is perpendicular section through monolayer at the level of row A or B. Lipids L, L, . . . L, are ionically linked by negative oxygen atoms to cations. All arrows in row C (+ → - bond) point in the same direction.

cations bound to lipids, as shown in the bottom vertical view. In free water such bonds are largely ionized. In the described situation, 3 lone electron pairs from neighbor water molecules, symmetrically oriented towards the cation should increase the stability of its electrostatic bond with the lipid. Occasional rupture of this bond, through thermal agitation or adverse transient ion fields, could still occur. If the intrinsic stability of this arrangement depended on the type of cation involved, the whole system would show selective properties. As seen in Figure 12, potassium, among monovalent cations, should feel particularly well at home in this complex.

The diagram shows the scaled up side and top views of the cation binding site where crystal radii dimensions (37) for the 3 participant water oxygen atoms W_1 , W_2 , and W_3 , for the negative oxygen atom L of the lipid, and for monovalent cations have been used. On the right is a view of section AB where dimensions appear in exact proportions. It is seen that the K ion fits particularly well and that very little distortion of the water network should occur through its presence. Other ions are either too big or too small. The smaller Na^+ and Li^+ ions, which are more readily hydrated (38), would tend to lean towards one of the 3 water molecules. The larger ions could not be ideally centered. In all cases save with K^+ , distortion of the lattice and decrease in intrinsic stability would occur. This would not be very pronounced for Rb^+ but would be so for Na^+ , and for Li^+ particularly. These conclusions are in good qualitative agreement with results obtained by Conway and Beary (39) on the relative affinity of various cations for the yeast cell membrane. The relative values found for the series K^+ , Rb^+ , Cs^+ , Na^+ , Li^+ were, respectively, 100;42;7;3.8;0.5. This would make the affinity for potassium $100/3.8 = 26.3$ times greater than for sodium.

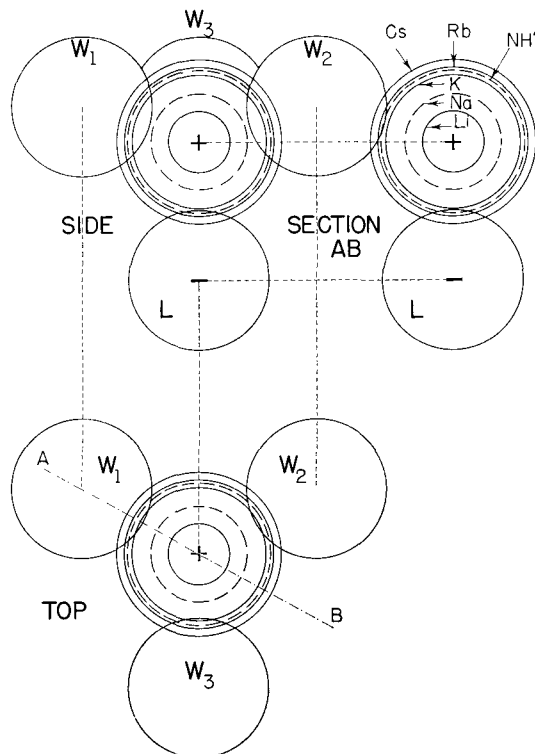


FIG. 12. Side view, top view and section AB of cation adsorptive site. Negatively charged lipid oxygen atom L is linked to cation. One water molecule in the water monolayer is exactly substituted by K^+ . If to this water molecule a proton is added instead, a OH_3^+ (hydronium) ion is formed (cf. Fig. 13).

On the other hand the dimensionally quite acceptable ammonium ion may be somewhat structurally handicapped. The hydronium ion, H_3O^+ is dimensionally very close to a water molecule and will fit very well. In fact (cf Figure 12 top view, with Figure 13) the 3 water molecules at the adsorptive site correspond exactly to the inner hydration shell described by Eigen (30). The mobility of the proton should, however, appreciably decrease the intrinsic stability of the hydrogen ion in this situation. Nevertheless, it should be clear that this ion would be readily formed at this site provided a proton could be supplied when needed. As shall be seen later, this need should arise in the normal process of cation transfer to and from the membrane. It is assumed that the protons are supplied by ATPase molecules located along the conductive pathway of water molecules just described.

A concept of fixed charges in a membrane should not come as a surprise in view of the work of Teorell (40), for example. Aschheim (41) even demonstrated that the adsorptive region is a thin monolayer, and both Eisenman (42) and Ling (43) considered the participation of water molecules necessary for cation selectivity. However, a simple comprehensive concept of the sodium pump and of the responsible structure was never proposed (44,45).

The Cation Pump

How does this system account for the specific asymmetry in K distribution found in many cellular systems? An example given on Figure 14 concerns the distribution of Na^+ and K^+ in human erythrocytes. To give a more striking idea of this distribution, the cation concns in the same volume, $V = 200,000 \text{ \AA}^3$, of the membrane, plasma and cytoplasm, have been represented. Note the small relative concn of K^+ in plasma and of Na^+ in the cell. Note also the relatively

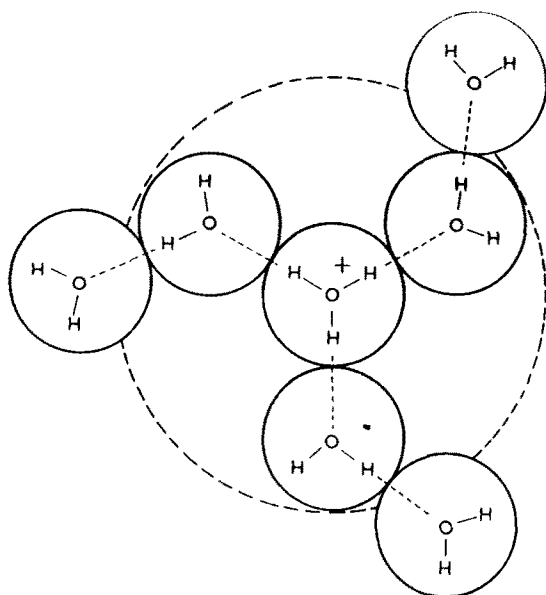


FIG. 13. Hydronium ion (center) surrounded by primary hydration shell (dashed circle) formed by three water molecules, according to Eigen (30). These molecules correspond to W_1 , W_2 , and W_3 in adsorptive site as seen in top view, Fig. 12. Molecules of secondary shell are also part of water monolayer.

low cation turnover, i.e., 0.5 per minute, indicating the remarkable stability of the system. It must be emphasized that although cations are appreciably more coned in the membrane, the number adsorbed could only represent a few per cent of the total number in the cell.

If we assume that Na and K ions are adsorbed in two distinct layers, the P-layer (near plasma) and the C-layer (near cytoplasm), and if we further assume a difference in cation adsorptive properties, then the K/Na ratio r of the number of sites occupied by the two cations in a layer at equilibrium can be expressed, using Langmuir's reasoning (46), for the P-layer,

$$r_P = \beta R_o \quad (1)$$

and the C-layer,

$$r_C = \beta R_i \quad (2)$$

where

$$\beta = a_K d_{Na} / d_{KNa} \quad (3)$$

is equivalent to the relative affinity defined by Conway and Beary (39) discussed above. Thus for the yeast cell, $\beta = 26.3$. R_o , R_i are the K/Na ratios of the outside and inside media (plasma and cytoplasm), respectively, and a_K , a_{Na} , the adsorption coefficients, and d_K , d_{Na} , the desorption coefficients for K^+ and Na^+ .

The simple relations (1) and (2) state that the K/Na ratio r is proportional to the activity ratio of the cations in the adjacent medium. From (1) and (2),

$$r_C = r_P R_i R_o^{-1} \quad (4)$$

This expression allows the calculation of r_C in the erythrocyte where $R_i = 5.15$ and $R_o = 0.03$ when $r_P = 1$. (If the value of β for the yeast cell is used in expression (1) with $R_o = 0.03$, one finds $r_P = 26.3 \times 0.03 \cong 0.8$ as a rough estimation of r_P for the erythrocyte). The value found, $r_C = 171$, clearly suggests that in the layer nearer the cytoplasm potassium must be in large excess. It is also possible to show that the cation composition of this layer would be relatively little affected by changes in the cation ratio R_o in plasma, while as shown by expression (1), such changes would be faithfully reflected in the P-layer.

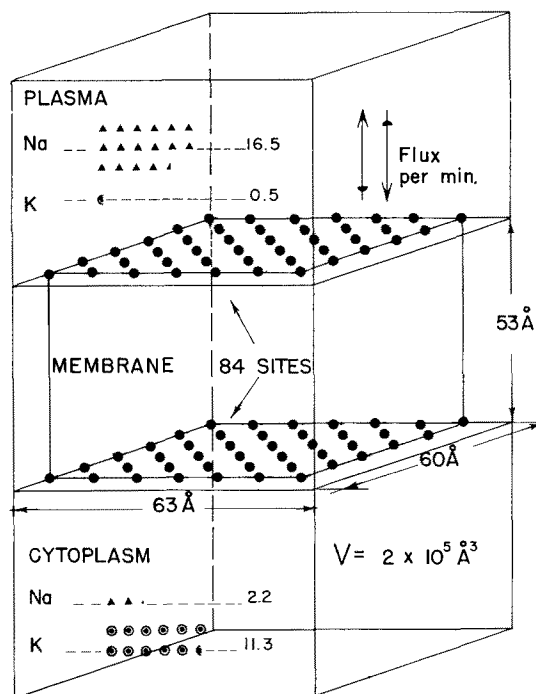


FIG. 14. Number of cations in equal volumes ($V = 2 \times 10^5 \text{Å}^3$) of plasma, of cytoplasm and of cationic region of erythrocyte membrane. The corresponding area includes $60 \times 63/90 = 42$ adsorptive sites in each cationic layer with 90Å^2 taken as approximate area occupied by each cholesterol-phospholipid complex. The (active) cation flux (see top right) is about 0.54/minute, calculated from the known value, 4×10^{-14} moles/sq. cm./sec. (47).

Figure 15 explains the Na-K disparity. Since electroneutrality requires that the number of charges be equal on both sides, the presence of immobilized negative charges (indicated by squares) on hemoglobin, Q , which is in the cytoplasm of the erythrocyte, will make the number of free-moving negative charges (indicated by circles) greater on the plasma side. The mobile charges are able to come close to the membrane and so create strong attractive fields promoting cation efflux. Thus if we started with an equal number of cations of both species on both sides, cation efflux would be much more active on the plasma side. Furthermore, this efflux would involve to a much larger extent the much less strongly adsorbed Na ions. Hence a larger number of cations, mostly Na^+ , would accumulate on the plasma side, building up a positive electrochemical potential tending to oppose further cation efflux and leading to an equilibrium. At this point the repulsive effect of accumulated Na ions would exactly compensate the attractive effect of mobile negative charges, and cation fluxes would become equal in both directions. The Na/K ratio disparity at equilibrium is thus readily explained by the combination of a disparity in the numbers of mobile negative charges (Donnan) with a dissimilarity in cationic adsorptive property.

According to the present view a net cation transfer from the P-layer to the C-layer and vice versa would only occur in favorable field situations such as those depicted in AB and CD, for example. The "pores," P (Figure 15), through which cations move in transit from one side of the membrane to the other are the long narrow spaces between the hydrocarbon chains of lipids which have been previously described (1) (see Figure 3). As their cross-sectional dimension and the condition for cation transfer described above suggest, movement in pores of more than one "naked"

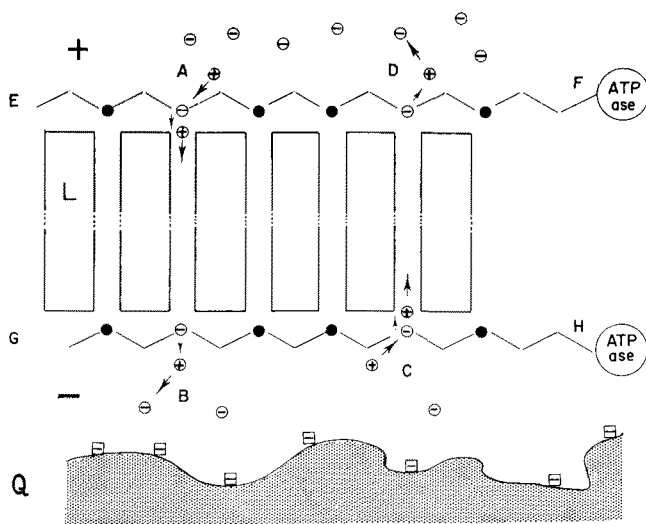


FIG. 15. Mechanism of cation exchange in erythrocyte. EF is conductive P (plasma side) layer; GH is conductive C (cytoplasm side) layer. L, L, . . . L represent lipids of bimolecular lipid leaflet where P, P, . . . P are "pores" (cf. Fig. 22, ref. 1). Q is hemoglobin in red cell cytoplasm where small squares represent fixed negative charges. Solid small circles in conductive layers are sites occupied by cations; open circles with - signs are sites temporarily unoccupied. Open circles, either in plasma or cytoplasm, are mobile charges (+ for cation, - for anions).

cation at a time, is excluded. At the adsorptive site, the temporary disturbance of water molecule orientation due to the occurrence of a negative charge is quickly counteracted by a proton supplied by ATPase activity, and moving along the conductive water molecule path. Bonting and Caravaggio have shown recently (47), that the Na-K dependent ATPase activity discovered by Skou (48) is directly and quantitatively correlated to Na and K active fluxes in many membranes. The correlation holds over a 25,000-fold range of activities, from the erythrocyte to the non-innervated Sachs organ of the electric eel, and corresponds to an average of 2.56 ± 0.19 cations per mole of hydrolyzed ATP.

The proposed system should work as long as a conductive pathway is maintained, i.e., as long as the necessary protons are supplied. ATPase activity thus appears as a maintenance device for the cation pump. Lack of this enzyme, lack of ATP fuel, inhibition of ATP production, inhibition of ATPase activity by such agents as ouabain (G-strophanthin), or by sodium or potassium deficiency, and several other causes would convert the system from an active to a simple diffusional process. Many membranes normally display a measure of passive cation movement. An interesting question is thus: Is this transport component due to the active system working at the limit of ATPase activity and leaking the rest of the time, or does it result from the existence of membrane regions where passive transport is a normal feature? Species differences in the proportions of passive and active areas would explain why, among mammals, cat, dog, sheep (49), and cow (50,51) erythrocytes do not show the striking reversal of the Na/K ratio displayed by those of horse, rabbit, monkey (49), dolphin (52), and man (53).

Membrane Potentials

These and other considerations explain why many observations (54-56), do not confirm an early theory correlating the resting potential with a Donnan-type equilibrium. A complete expression of this potential

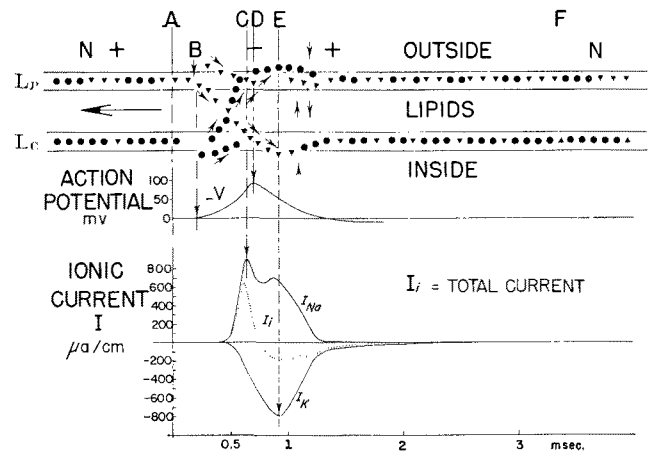


FIG. 16. Pictorial representation of cation fluxes (circles = K, triangles = Na) in the course of a nerve impulse. These are synchronized with action potential and ionic current curves obtained by Hodgkin and Huxley (62). The impulse, travelling from right to left, has reached point A of a still undisturbed region N; the disturbance and eventual recovery which occur in its wake are depicted by movements of cations in the directions shown by arrows. L_p and L_c are P layer and C layer, respectively.

must include important components related to ionic currents.

In the present concept the origin of these currents lies in the cation turnover of the adsorptive layers. This random phenomenon simultaneously provides free cations in one layer and empty sites in the other. Transfer occurs only when the two events happen to coincide in time and to correspond in space. Since ionic currents must equalize at equilibrium, the slow turnover rate of the K-rich, Na-poor C-layer sets the pace of ionic transfer within the membrane. Because the cation composition of the C-layer is less affected by changes in external cation activity, this layer must exert a moderating influence on ionic currents which explains the observed relative independence of the resting potential from moderate changes in external cation composition (57,58).

Figure 16 gives a pictorial interpretation of the sequence of events during the propagation of a nerve impulse. These events affect successively all sections of the nerve membrane as soon as a wave of depolarization reaches any point A of the membrane in its resting state N. These events all take place in a few milliseconds and are followed by restoration of the normal state, N, during a relatively long recovery period terminated at F. The movements of Na⁺ and K⁺ ions in the two adsorptive layers of the membrane are shown synchronized with the action potential and ionic current curves obtained by Hodgkin and Huxley (62) in their outstanding work on the giant squid axon, *Loligo forbesi* (58-62). One thus observes, after a brief period AB, an intense movement of ions in both directions, the ions primarily moving down their electrochemical gradients. To the outside observer, the first event occurring at B would be a net inward movement of sodium ions culminating at C, at which point a net outward potassium flux, culminating at E will be manifested. From this point on, the cation pump system slowly regains control and the adsorptive layers are reorganized.

One need not go into further detail to demonstrate that a development of the present structural concept will not come in conflict with the results obtained by Hodgkin and Huxley. However, it may lead to redefining the physical significance of some parameters

TABLE I
Amino Acid Composition of Myelin Protein*
(A = number per 100 residues)

Residue	A	Totals	Residue	A	Totals
Lysine	5.75	Cationic 12.00	Glycine	10.87	Aliphatic 40.79
Histidine	2.30		Alanine	9.65	
Arginine	3.95		Valine	5.91	
		Ionic	Leucine	8.76	
		32.19	isoLeucine	4.52	
			Methionine	1.08	
Aspartic	6.13	Anionic 20.19	Phenylalanine	4.02	Cyclic 10.21
Glutamic	7.14		Tryptophan	5.08	
Tyrosine	3.14			Proline	1.11
Cysteine	3.78				
Threonine	6.41	Hydroxyl 16.81			
Serine	10.40				
POLAR		49.00	APOLAR		51.00

*Calculated using data from Hulcher (6).

appearing in their equations. This is to be expected in any event, since these equations, which so remarkably describe the course of events in nerve impulse propagation, are basically empirical and were designed without specific structural background.

It has been observed that the propagation of the cation potential is a self sustaining, all or none phenomenon. It should be evident that the triggering event must be much more extensive than the disturbance caused by a single cation transfer. This event should so upset the adsorptive monolayer that the number of cations simultaneously released in the disturbed area becomes too large to allow a rapid ATPase-induced restoration of the normal order. The local upset can then extend unchecked beyond the initial disturbance, giving rise to further massive cation movement. In this way, a wave of excitation travelling ahead of an active cation release would be started. The propagation of a nerve impulse therefore depends on the pre-existence of two unbroken, fully loaded conductive monolayers, and on the initiation of a local stimulation of sufficient magnitude. It is known that such excitation may be obtained mechanically, i.e., by injury (disruption of the conductive layer) or by electrical depolarization when the "threshold current" is exceeded.

The size of such current, over and above the threshold value, should have little effect on the speed of propagation and the magnitude of ion currents (action potential) following stimulation. From Figure 16, it is possible to understand that action potential V is governed by the difference in net cation fluxes at the peak of disturbance. As Hodgkin and Huxley pointed out (62), the size of the net sodium current determines this difference. It should be possible therefore to increase the action potential by decreasing r_p , i.e., by decreasing R_o , the K/Na activity ratio on the plasma side. Conversely, the action potential should decrease with an increase of this ratio or its decrease on the other side of the membrane. While these phenomena are actually observed, a sufficient increase in K concn on the plasma side should so decrease the Na content of the P-layer that the depolarization required for the initiation of an action potential could not set in. In addition, the overall stability of a K-rich P-layer would be too large for a local disturbance to be propagated (potassium block). On the other hand, a large increase in internal Na concn should decrease the stability of the C-layer, and consequently that of both layers, to the point where the fully loaded conductive monolayers necessary for impulse propagation are no longer maintained. This is also true during the refractory period AN. The above and other observed phenomena are readily explained by the twin adsorptive layers concept. It has been shown that the latter also ex-

plains active transport without relying on a complex array of specific carriers, enzymes and selective compounds for the existence of which there is no unassailable evidence (63). However, the principal merit of this plausible structural and functional role of water may be that it suggests the existence of a largely unexplored yet undoubtedly fruitful field of investigation.

Discussion

Myelin does not appear to be an active system since Shanes (64) has shown that the K/Na ratio merely reflects that of the surrounding endoneurium. The role of myelin would appear to be that of an insulator decreasing the electric leakage of the axon which it surrounds, thereby increasing the speed of impulses. Judging from the wasting effect of demyelinating diseases, this role is obviously a very important one. On the other hand, the process of myelination would appear to involve the elimination of superstructural elements which account for specialized functions of membranes, and were undoubtedly present in the glial cell membrane from which myelin originated. The simplified unit only includes lipids, water, ions, and a thin layer of structural protein. This basic feature, probably common to all membranes, would appear to be a distinct structural entity to which functional elements confer the status of a complete membrane (Figure 2, II). It is important to establish this distinction for, in attempting to resolve the structure of membranes one could be misled in equating superstructural protein elements with the structural protein of the simple "lipoprotein barrier."

From the multilayer arrangement described in Figures 11 and 12, ref. 1, and from the present concept of unit layer structure (Figure 3), it is possible to understand that only the relatively small proportion of total lipids located in the external layer could readily exchange with lipids synthesized by the glial cell. While this condition accounts for the slow overall turnover rate of mature myelin lipids observed by Davison (65), the existence of a very slow diffusional process involving permutation of lipids within the bimolecular leaflet cannot be excluded. If this led to exchange of external lipids with those in deep-seated layers, the compositional changes in aging and disease would reflect alterations in the lipid metabolism of glial cells.

So far, wide angle X-ray diffraction studies of myelin have revealed only two rather diffuse reflections, the first at about 10 Å, the other spreading from 4.6 to 4.9 Å. The latter roughly corresponds to the widest cross-sectional dimension of lipid chains; free myelin lipids in bulk give a similarly located diffuse reflection. In view of a possible correspondence of protein and lipid parameters indicated above, the two reflections may not necessarily have the same origin. In any case, these wide angle data do not constitute specific evidence of a disorderly state of the lipid chains (9). Yet this view has been accepted by some authors or is at least implicit in their views of membrane structure (66). Since the bulk free lipids form a liquid mixture it has been assumed that the configurational distribution of chains is similar to that found in liquid hydrocarbons, although the only available data concern relatively short chain ($C \leq 7$) molecules. The latter, as shown by infrared spectroscopy (67), do display a relatively wide configurational spectrum. On the other hand, the long chain polar lipids are remarkable in their ability to

form micelles and monolayers, a property which manifests itself when chains exceed 12 carbon atoms in length. While this is readily explained in terms of molar van der Waals interchain interaction, the transition is much sharper than would be expected from a simple proportionality to chain length. This effect probably involves a simplification in configurational variability which further increases the tendency to form low entropy associations. In crystalline saturated lipids, this effect leads to the chains adopting a single type of configuration (68). It is thus probable that the long chains in bulk polar lipids are far more restricted as to the range of configurational distribution than has been assumed. Liquid-crystalline lipid systems have shown that a mere ability to flow is not restricted to true liquids, nor is it necessarily indicative of a disorderly state of molecules.

Poor definition in the wide angle X-ray patterns of myelin need not indicate disorder in lipid chain configuration. No matter how orderly the lipid complex arrangement and the complex pattern in any one layer, these would not be reproduced in adjacent or successive layers. The complex units differ individually, both in the type of lipid associated with cholesterol and in their orientation about their main axes (1). Such features represent a basic difference with tridimensionally symmetrical crystalline lattice, preventing X-ray diffraction from supplying detailed information on the order existing in any one layer or on all but the most consistent geometrical features of the system as a whole. Among the latter, the parallelism of regularly spaced planes containing the phosphorus atoms is clearly revealed by low angle diffraction techniques (9). The 10 Å wide angle reflection, apparently unrelated to lipid dimensions, possibly corresponds to the 9.8 Å spacing of protein chains proposed in the present model.

The tertiary structure of myelin protein is a matter of considerable theoretical interest. The presence of proline residues (Table I) indicates that chains of individual protein molecules are not uniformly straight and must consist of several straight sections. They could, for instance, form flat spirals within the HPr planes (Figure 3) and parallel to the surface of the lipids. Stereomodels show this arrangement to be compatible with the present concept. If the approximate mol wt, 10,000, of myelin protein molecules (69), is taken into account such coils are formed of approx 330 Å long chains (about 100 residues, one every 3.3 Å) and their diameter would be about 60 Å, assuming a regular 9.8 Å intrachain spacing within coils. With the normal complement of associated lipids, each coil would constitute a lipoprotein particle of about 45,000 mol wt. Since no modification of the proposed lipid leaflet arrangement is required to account for this protein structure, the model appears entirely compatible with a "particulate" concept of the membrane. An interesting aspect of this theory results if one assumes that some of the bonds between individual coils will differ enough from bonds within coils to account for the lipoprotein particles behaving as a unit under specific circumstances. Wandering molecules adsorbed from the extracellular fluid and capable of modifying intercoil binding forces could promote local alterations of particle positions leading to molecular penetration into the cell. This would account for the transport of many solutes appearing to be enzymatically directed. For indeed, transfer through the membrane would then

depend on specific properties of bonds and adsorbed solute, subjected to blocking and competitive inhibitions. Furthermore, the kinetics would follow the laws of adsorption, i.e., would be represented by Langmuir isotherms which are formally identical to the Michaelis-Menten equation (70). In many respects, the behavior postulated for "permeases" (71) or "transportases" (72) would be observed. This principle could apply to pinocytosis, facilitated transport, and even active molecular transport, without invoking the existence in membranes of an extensive array of transport enzymes and carriers (73). In the course of transport, the local parting of unit particles could involve the rupture of the conductive monolayer described above with attendant local movement of Na and K ions. Induced activity of the ATPase unit then would lead to restoration of monolayer conductivity. Correlations of cation and molecular transfer have indeed been observed (74,75). A unified concept of transport (76) centered on the properties of a conductive water monolayer thus appears possible.

REFERENCES

1. Vandenheuvel, F. A., *JAOS* 40, 455 (1963).
2. Jackson, H. R., and F. A. Vandenheuvel, *J. Photog. Sci.* 12, 134 (1964).
3. Vandenheuvel, F. A., Symposium on Demyelinating Diseases, New York Acad. Sci., New York, Jan. 1964.
4. Geren, B. B., *Exp. Cell Res.* 7, 558 (1954).
5. Robertson, J. D., *Biochem. Soc. Symposia* (Cambridge, England) 16, 3 (1959).
6. Hulcher, F. H., *Arch. Biochem. Biophys.* 100, 237 (1963).
7. Laatsch, R. H., S. Gordon, M. W. Kies and E. C. Alvord, Jr., *Federation Proc.* 20, 343 (1961).
8. Autilio, L., W. T. Norton and R. Terry, Symposium on Demyelinating Diseases, New York Acad. Sci., New York, January, 1964.
9. Finean, J. B., *Circulation* 26, 1151 (1962).
10. Finean, J. B., Symposium on Demyelinating Diseases, New York Acad. Sci., New York, January, 1964.
11. Danielli, J. E., *J. Cell. Comp. Physiol.* 5, 495, (1935).
12. Schmidt, W. J., *Z. Zellforsch.* 23, 657 (1936).
13. Schmitt, F. O., R. S. Bear and K. J. Palmer, *J. Cell. Comp. Physiol.* 18, 3 (1941).
14. Dervichian, D. G., "Surface Phenomena in Chemistry and Biology," Pergamon Press, New York, 1958, p. 70.
15. Van Deenen, L. L. M., U. M. T. Houtmuller, G. H. de Haas and E. Mulden, *J. Pharm. Pharmacol.* 13, 670 (1962).
16. Marsh, R. E., L. Pauling and R. B. Corey, *Biochim. Biophys. Acta* 16, 1 (1955).
17. Finean, J. B., *J. Biophys. Biochem. Cytol.* 8, 13 (1960).
18. Joy, R. T., and J. B. Finean, *J. Ultrastruct. Res.* 8, 864 (1963).
19. Kates, M. L., S. Yengoyan and P. S. Sastry, *Biochem. Biophys. Acta*, in press (1964).
20. Kushner, D. J., S. T. Bayley, J. Boring, M. Kates and N. E. Gibbons, *Canad. J. Microbiol.* 10, 463 (1964).
21. Szent-Györgyi, A., "Bioenergetics," Academic Press, New York, 1957, p. 89.
22. Szent-Györgyi, A., *Nature* 148, 157.
23. Green, D. E., and S. Fleischer, "Horizons in Biochemistry," Ed. Kasha, M., and B. Pullman, Academic Press, London, 1962.
24. Fernández-Moran, H., "Ultrastructure and Metabolism of the Nervous System, Vol. XL Res. Publ. Assoc. Res. Nervous Mental Disease, 1962, p. 266.
25. Eley, D. D., "Horizons in Biochemistry," Ed. Kasha, M., and B. Pullman, Academic Press, London, 1962, pp. 361-368.
26. King, G., and J. A. Medley, *J. Colloid Sci.*, 4, 1, 9 (1949).
27. Eley, D. D., G. D. Parfitt, M. J. Perry and D. H. Taysum, *Trans. Faraday Soc.* 49, 79 (1953).
28. Riehl, N. V., *Naturwissenschaften* 43, 145 (1956).
29. Riehl, N. V., *Kolloid-z.* 151, 66 (1957).
30. Eigen, M., "Hydrogen Bonding," Ed. Hazi, D., and H. W. Thompson, Pergamon Press, New York, 1957, p. 429.
31. Klotz, I. M., "Horizons in Biochemistry," Ed. Kasha, M., and B. Pullman, Acad. Press, London, 1962, p. 528.
32. Mecke, R., and W. Baumann, *Physik. Z.* 33, 833 (1932).
33. Darling, B. T., and D. M. Dennison, *Phys. Rev.* 57, 128, (1940).
34. Posener, D. W., and M. W. P., *Stranberg, Ibid.* 95, 374 (1954).
35. Peterson, S. W., and H. A. Levy, *Acta Cryst.* 10, 70 (1957).
36. Pauling, L., "The Nature of the Chemical Bond," 3rd ed., Cornell University Press, New York, 1960, p. 465.
37. Pauling, L., *Ibid.*, p. 518.
38. Audubert, R., and S. de Mende, "The Principles of Electro-phoresis," Hutchinson, London, 1959, p. 10.
39. Conway, E. J., and M. E. Beary, *Biochem. J.* 69, 275 (1958).
40. Teorell, T., *Exp. Cell Res. suppl* 5, 1958; Academic Press Inc., New York, 1958, pp. 83-100.
41. Ascheim, E., "Membrane Transport and Metabolism," Ed. Kleinzeller, A., and A. Kotyk, Academic Press, London, 1960, p. 155.
42. Eisenman, G., *Ibid.*, pp. 163-179.
43. Ling, G., *J. Gen. Physiol.* 43, suppl. 149.
44. Davies, R. E., "Membrane Transport and Metabolism," Ed. Kleinzeller, A., and A. Kotyk, Academic Press, London, 1960, p. 320.
45. Davies, R. E., and R. D. Keynes, *Ibid.*, p. 336-340.
46. Langmuir, I., *J. Am. Chem. Soc.* 38, 2267 (1916).
47. Bonting, S. L., and L. L. Caravaggio, *Arch. Biochem. Biophys.* 101, 37 (1963).
48. Skou, J. C., *Biochem. Biophys. Acta* 23, 394 (1957).
49. Bernstein, R. E., *Science* 120, 459, (1954).
50. Martin, F. N., Jr., *New Orleans M. S. J.* 99, 103 (1946, 1947).
51. Duncan, C. W., C. F. Huffman and G. C. Gerritsen, *Michigan Agr. Exp. Sta.*, 1959, unpublished.
52. Eichelberger, L., E. S. Fletcher, Jr., E. M. K. Geeling and B. J. Vos, Jr., *J. Biol. Chem.* 133 (1940).

53. Overman, R. R., and A. K. Davis, *Ibid.* 168, 641 (1947).
 54. Curtis, H. J., and K. S. Cole, *J. Cell. Comp. Physiol.* 19, 135 (1942).
 55. Hodgkin, A. L., *Biol. Rev. Cambridge Philos. Soc.* 26, 339, (1951).
 56. Bolingbroke, V., and M. Maizels, *J. Physiol. (Lond.)* 149, 563 (1959).
 57. Grunfest, H., "Electrochemistry in Biology and Medicine," Ed. Shedlovsky, T., John Wiley and Sons, Inc., New York, 1955, p. 141.
 58. Hodgkin, A. L., A. F. Huxley and B. Katz, *J. Physiol. (Lond.)* 116, 424 (1952).
 59. Hodgkin, A. L., and A. F. Huxley, *Ibid.* p. 473.
 60. Hodgkin, A. L., and A. F. Huxley, *Ibid.* p. 449.
 61. Hodgkin, A. L., and A. F. Huxley, *Ibid.* p. 497.
 62. Hodgkin, A. L., and A. F. Huxley, *Ibid.* 117, 500 (1952).
 63. Judah, J. D., and K. Ahmed, *Biol. Rev.* 39, 169 (1964).
 64. Shanes, A. M., "The Biology of Myelin," Ed. Korey, S. R., Hoeber-Harper, New York, 1959, p. 173.
 65. Davison, A. N., Symposium on Demyelinating Diseases, New York Acad. Sc., New York, January, 1964.
 66. Stoekenius, W., "The Interpretation of Ultrastructure," Academic Press, New York, 1961, p. 349.
 67. Chapman, D., Symposium on Quantitative Methodology in Lipid Research, Penn State University, August, 1964.
 68. Chapman, D., *Chemical Reviews* 62, 433 (1962).
 69. Thompson, E. B., and Marian W. Kies, Symposium on Demyelinating Diseases, New York Acad. Sci., January, 1964.
 70. Willbrandt, W., "Membrane Transport and Metabolism," Ed. Kleinzeiler, A., and A. Kotyk, Academic Press, New York, 1961, p. 388.
 71. Cohen, G. N., and J. Monod, *Bact. Rev.* 21, 169 (1957).
 72. Sois, A., *Bull. Soc. Chim. Biol.*, 39, suppl. II, 3.
 73. Mitchell, P., "Membrane Transport and Metabolism," Ed. Kleinzeiler, A., and A. Kotyk, Academic Press, New York, 1961, p. 22.
 74. Crane, E. K., D. Miller and I. Bihler, *Ibid.* p. 439.
 75. Quastell, J. H., *Ibid.* p. 512.
 76. Christensen, H., *Ibid.* p. 510.

Lipid Class and Fatty Acid Composition of Intact Peripheral Nerve and During Wallerian Degeneration

J. F. BERRY, W. H. CEVALLOS,¹ and R. R. WADE, JR., Division of Neurology
 University of Minnesota, Minneapolis

Abstract

Lipid extracts from normal cat, chicken, and beef sciatic nerve were fractionated into their components by combinations of silicic acid, Florisil, DEAE-cellulose, or silicic acid-silicate column chromatography.

The constituent fatty acids of total lipid extracts and of individual lipid classes were qualitatively and quantitatively determined as their methyl esters by gas chromatography.

These methods were also applied to lipid extracts from cat sciatic nerve undergoing Wallerian degeneration at 8, 16, 32, and 96 days after section and to chicken sciatic nerve undergoing demyelination due to organophosphate poisoning.

All fatty acids were markedly decreased in the total lipids of cat sciatic nerve at 96 days after section and most of these were decreased at 32 days. As early as 8 days after section 16:0, 16:1, 18:2, 20:0, and 20:4 showed decreases, while 18:0, 18:1, 22:1, 22:5, 22:6, and 24:1 did not begin to show decreases until 16 days after section. The decreases in fatty acids were considered to be due to increased catabolism, decreased synthesis, or increased removal of fatty acids from nervous tissue. The fatty acid content of the total lipids of chicken nerve undergoing demyelination resembled that of cat sciatic nerve between 16 and 32 days after section.

Myelin lipids, sphingomyelin, cerebroside, and phosphatidyl ethanolamine (PE) began to decrease as early as 8 days after section in cat sciatic nerve. Phosphatidyl serine (PS) also decreased at this time. Cholesterol, lecithin, and ethanolamine plasmalogen did not begin to decrease until 16 days after section and phosphatidyl inositol (PI) did not decrease until 32 days after section. Triglycerides decreased markedly at 8 days after section gradually returning to normal by 96 days. This was accompanied by a transient increase in free fatty acids and monoglycerides. Cholesterol esters and lysolecithin increased markedly at 8 days after section and were higher than normal levels even at 96 days after section.

In chicken sciatic nerve undergoing demyelination after organophosphate poisoning, cerebroside was the only myelin lipid which decreased in amt, while cholesterol esters and diglycerides increased.

Sphingomyelin and cerebroside containing 16:0, 18:0, 18:1, 18:2, 20:0, 22:0, 23:0, 24:0, 24:1 seemed to be most susceptible to degradation or interference in synthesis in degenerating nerve. For the most part, these fatty acids were observed to increase in cholesterol esters, free fatty acids, and, in some instances, triglycerides.

The changes in various lipid classes and their constituent fatty acids are discussed in relation to various cellular changes which accompany degeneration.

Introduction

THERE ARE DESCRIBED in the literature many detailed studies of the lipid compositions of brain in various animal species and in recent years increasing attention has been focussed on such studies making use of modern methods of lipid chemistry. However, there are relatively few reports on the lipid composition of peripheral nerve. Studies on peripheral nerve are of interest because an experimental peripheral nerve demyelination which follows a reproducible course can be induced in laboratory animals by a relatively simple operative procedure.

Early studies on the lipid composition of peripheral nerve were reported by Falk (1), Randall (2), Schmidt et al. (3), Johnson et al. (4), Brante (5), and a more recent study by McCaman and Robins (6). These investigations all made use of indirect procedures involving hydrolysis of lipids with subsequent colorimetric estimation of water-soluble hydrolysis products. The only reports involving isolation of lipids are those of Webster on the plasmalogen, cephalins, lecithin, sphingomyelin, and lysolecithin content of sciatic nerve (7,8).

Classical studies on the lipid composition of a peripheral nerve undergoing Wallerian degeneration are those of Johnson et al. (9), Burt et al. (10), and of Brante (5). These authors applied the terms "myelin lipids" and "sheath typical lipids," respectively, to describe the group of lipids which decline rapidly in conen in degenerating nerve (cholesterol, cerebroside, sphingomyelin). McCaman and

¹Biochemistry Research Division, Sinai Hospital of Baltimore, Inc., Baltimore, Md.